

# Perturbative analysis of the conductivity in disordered monolayer and bilayer graphene

Andreas Sinner and Klaus Ziegler

*Institut für Physik, Universität Augsburg*

(Received 13 October 2011; published 1 December 2011)

The DC conductivity of monolayer and bilayer graphene is studied perturbatively for different types of disorder. In the case of monolayer, an exact cancelation of logarithmic divergences occurs for all disorder types. The total conductivity correction for a random vector potential is zero, while for a random scalar potential and a random gap it acquires finite corrections. We identify the diagrams which are responsible for these corrections and extrapolate the finite contributions to higher orders which gives us general expressions for the conductivity of weakly disordered monolayer graphene. In the case of bilayer graphene, a cancelation of all contributions for all types of disorder takes place. Thus, the minimal conductivity of bilayer graphene turns out to be very robust against disorder.

DOI: [10.1103/PhysRevB.84.233401](https://doi.org/10.1103/PhysRevB.84.233401)

PACS number(s): 81.05.ue, 72.80.Vp, 72.10.Bg

**Introduction.** Monolayer graphene (MLG) represents a monoatomic sheet of carbon atoms arranged in a honeycomb lattice with lattice spacing  $a$  and next-neighbor hopping energy  $t \approx 2.8$  eV. The transport properties of charge-neutral MLG are characterized by the semimetallic behavior with a point-like Fermi surface at two nodes (valleys) and linear low-energy dispersion in the vicinity of these valleys. This remarkable fact is one reason for the outstanding electronic properties of ML graphene.<sup>1-3</sup> Perhaps the most prominent transport property of ML graphene is the minimal conductivity  $\bar{\sigma}_0 = e^2/h\pi$  exactly at the Dirac point which has been observed in a number of experiments.<sup>1,2,4</sup> Bilayer graphene (BLG) represents two ML honeycomb lattices with Bernal stacking, where the interlayer hopping processes are allowed with the energy  $t_\perp \approx 0.4$  eV. The main difference between MLG and BLG is that the low-energy excitations of the latter have a quadratic spectrum in the vicinity of the valleys.<sup>5</sup> This difference causes a factor of two for the DC conductivity  $\bar{\sigma}_0 = 2e^2/h\pi$ . Experimentally, both values seem to depend only very weakly on disorder or thermal fluctuations,<sup>5-9</sup> which is supported by field-theoretical studies for various types of disorder.<sup>10-16</sup>

To the best of our knowledge, a systematic diagrammatic analysis of the conductivity of disordered graphene has not been performed so far. Usually, only certain types of diagrams are taken into account. Such approximations cannot be considered as fully controllable, since each diagram in the perturbative expansion exhibits logarithmic divergences. Therefore, the final result of calculations must crucially depend on a correct counting of diagrams. It is the purpose of this paper to demonstrate this for the conductivity calculated within the Kubo formalism.

**Kubo formula.** Within the linear response theory, the conductivity of graphene per a spin and valley projection can be approximated for low frequencies ( $\omega \sim 0$ ) by the Kubo formula<sup>17</sup>

$$\bar{\sigma}(\omega) = -\omega^2 \frac{e^2}{2h} C_g(\omega), \quad (1)$$

where

$$C_g(\omega) = \sum_r r_k^2 \text{Tr} \left( G_{r0} \left( i\epsilon + \frac{\omega}{2} \right) G_{0r} \left( -i\epsilon - \frac{\omega}{2} \right) \right)_g \quad (2)$$

is the analog of the (mean square) displacement function of a classical random walk. The spin-valley degeneracy should be taken into account by multiplying it with an additional factor 4. The symbol  $r_k$  denotes the  $k$  component of the position operator; the brackets  $\langle \dots \rangle_g$  mean average with respect to disorder of strength  $g$ . The expression  $G_{rr'}(z)G_{r'r}(-z)$  is referred to as the two-particle Green's function and is commonly depicted diagrammatically as a closed loop . Here,  $G$  denotes the one-particle Green's function with

$$G^{-1}(z) = \hbar z + \sigma \cdot \nabla + v^2 \hat{u}_r, \quad (3)$$

where the vector  $\sigma$  consists of Pauli matrices  $\sigma_{1,2}$  and  $\hat{u}_r$  represents a disorder potential. The operator of kinetic energy reads  $\nabla_i = i\hbar v \partial_i$  for MLG with the Fermi velocity  $v = \sqrt{3}ta/2\hbar$ , and  $\nabla_1 = \hbar^2(\partial_1^2 - \partial_2^2)/2\mu$  and  $\nabla_2 = \hbar^2 \partial_1 \partial_2 / \mu$  for BLG, where  $\mu = 2t_\perp \hbar^2 / 3t^2 a^2$  denotes the electron band mass. For BLG, we also define a characteristic velocity  $v = \hbar/a\mu = 3t^2 a / 2t_\perp \hbar$  which appears in the Green's function. Here, we consider three disorder types: 1) random scalar potential,  $\hat{u}_r = V_r \sigma_0$ ; 2) random vector potential  $\hat{u}_r = \sigma \cdot A_r$ ; and 3) random gap  $\hat{u}_r = \delta M_r \sigma_3$ . We assume disorder to be Gaussian correlated with zero mean, i.e.,  $\langle \hat{u}_r \rangle = 0$ ,  $\langle \hat{u}_r \hat{u}_{r'} \rangle = (\hbar/v)^2 (g/mv^2) \delta(r-r')$  ( $\langle \hat{u}_r \hat{u}_{r'} \rangle = (\hbar/v)^2 (g/mv^2) \delta_{ij} \delta(r-r')$  for random vector potential), with corresponding  $v$  and  $m = m_e$ , the bare electron mass for MLG ( $m_e v^2 \approx 6$  eV), and  $m = \mu$  for BLG ( $\mu v^2 \approx 30$  eV). Our assumption suggests  $g/(mv^2) \ll 1$ . Below we use a unit system with  $\hbar = 1$ ,  $e^2/h = 1$ ,  $m_e = 1$ ,  $2\mu = 1$ , and  $v = 1$ .

Before we embark on the perturbative calculation, we briefly discuss the status quo of the field-theoretical approach. In the case of a random vector potential, representing random ripples in graphene, a bosonized replica approach yields for MLG  $\bar{\sigma} = \bar{\sigma}_0$ .<sup>11</sup> The random gap case is of particular interest, because it describes a metal-insulator transition due to the opening of the gap  $m$ . The displacement function  $C_g(m, \omega)$  can be evaluated in this case by replacing the random field  $\delta M_r$  by a more general random field. This mapping enables us to search for saddle points in a multidimensional manifold. It turns out that not just a single saddle point exists but a whole saddle-point manifold. As a result, we have one massless mode.<sup>14</sup> The latter creates an  $\omega^{-2}$  singularity in  $C_g(m, \omega)$ , which cancels the  $\omega^2$  factor in the conductivity of Eq. (1). There

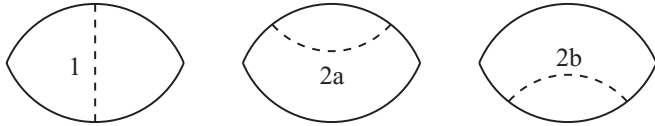


FIG. 1. Two-loop corrections of the two-particle Green's function. Each diagram appears twice in the expansion. Solid lines in the upper/lower bow correspond to Green's functions of clean graphene ( $\hat{u} = 0$ )  $G(-z)/G(+z)$  and slashed lines to the disorder.

are also massive modes around the saddle-point manifold. Altogether this leads to the following scaling form:

$$C_g(m, \omega) = \frac{(\omega + 2i\eta)^2}{\omega^2} C_0(m/2, \omega + 2i\eta) K_g, \quad (4)$$

with the displacement function of the pure system

$$C_0(m, \omega) = \frac{2}{\pi} \frac{1}{4m^2 - \omega^2}. \quad (5)$$

$K_g$  is the contribution of the massive modes. Although its form is unknown for  $g > 0$ , it is always finite with  $K_0 = 1$  for  $g = 0$ . The scattering rate  $\eta$  is given by  $\eta = (m^2 - m_c^2)\Theta(m_c^2 - m^2)/4$  with  $m_c = \Lambda e^{-\pi/g}$ .<sup>14</sup> It should be noticed that the  $\omega^{-2}$  singularity of  $C_g$  disappears for both MLG and BLG for  $\eta = 0$  and  $m > 0$ . In terms of the conductivity of Eq. (1), this yields for  $\omega \sim 0$  eventually

$$\bar{\sigma} \sim \bar{\sigma}_0 K_g \left(1 - \frac{m^2}{m_c^2}\right) \Theta(m_c^2 - m^2). \quad (6)$$

This result indicates that  $\bar{\sigma}$  vanishes for any  $m > 0$  in perturbation theory because  $m_c$  is always zero in the latter. On the other hand, for  $m = 0$  the perturbation theory should reproduce  $\bar{\sigma} = \bar{\sigma}_0 K_g$ , since the  $m_c$  drops out of the conductivity in this case.

*Perturbative theory.* Now we evaluate the displacement function perturbatively in powers of the disorder strength  $g/2$ . In order to perform these calculations, the translational invariance broken by disorder has to be restored by averaging over the Gaussian ensemble. Here, we perform this averaging using a diagrammatic representation. The first order conductivity corrections arise from the graphs depicted in Fig. 1. Results of the evaluation of these diagrams are shown in Table I, where we only retain constant contributions and logarithmically divergent terms. The second-order (three-loop order) diagrams contributing to the conductivity are shown in Fig. 2 and results of their evaluation are summarized in Table II. Technical details of the evaluation can be found in the supplementary material.<sup>18</sup> The total combinatorial factor for each topological class of diagrams is  $2^n$ . Each topological class of diagrams exhibits in turn further degeneracy due to

diagram symmetries: The degeneracy factor of the first-order topological class 1 (Fig. 1) and of the second-order topological classes 1, 2, and 7 (Fig. 2) is one, while that of the first-order topological class 2 (Fig. 1) and of the second-order topological classes 4, 5, 6, and 8 (Fig. 2) is two and degeneracy factor of the second-order topological class 3 is four. All these factors should be carefully taken into account.

First we discuss results for monolayer graphene. To the two-loop order, contributions to the displacement function from all diagrams reveal divergences  $\sim \omega^{-2} \ln \Lambda/\omega$ . Here,  $\Lambda$  denotes the UV cutoff and  $\omega$  the imaginary frequency in contrast to Eqs. (1) and (2). The emergence of the logarithms is due to the divergence of the loop integrals

$$I = \int \frac{d^2k}{(2\pi)^2} G_k(z) \sim \ln \frac{\Lambda}{\omega}, \quad (7)$$

while the singularity  $\omega^{-2}$  appears in the displacement function due to rescaling of the factor  $r_k^2$  in Eq. (2),<sup>18</sup> but disappears in the conductivity because of the factor  $\omega^2$  in Eq. (1), as in the field-theoretical approach discussed above. At the three-loop level, contributions from diagrams containing intercrossing impurity lines (diagrams 6, 7, and 8 in Fig. 2) vanish after angular integration. Contributions to the displacement function arising from each diagram with noncrossing impurity lines diverge  $\sim \omega^{-2} (\ln \Lambda/\omega)^2$ , with some of them revealing subdominant divergence  $\sim \omega^{-2} \ln \Lambda/\omega$ . However, to both orders  $g$  and  $g^2$ , the sum over all conductivity contributions is finite, i.e., singularities to both orders  $\sim \ln \Lambda/\omega$  and  $\sim (\ln \Lambda/\omega)^2$  cancel each other exactly. For the random vector potential, the conductivity correction is zero to both two- and three-loop order. This is in accord with the findings of Refs. 11, 15, and 16. For random gap and random scalar potential to both orders, finite conductivity corrections are generated only by ladder diagrams, i.e., by diagrams 1 in Figs. 1 and 2. Provided that the cancelation of singularities holds to higher orders as well, the analysis of higher order ladder diagrams yields the following general expression for the  $n$ th order ( $n \geq 1$ ) conductivity correction

$$\bar{\sigma}_0 \frac{(\pm 1)^n}{2^{n-1}} \left(\frac{g}{2\pi}\right)^n, \quad (8)$$

with  $+$  for the random scalar potential and  $-$  for the random gap. This expression has been verified to the fourth order in perturbative expansion (five-loop order). The sum over  $n \geq 1$  converges and we obtain for the conductivity

$$\bar{\sigma}_{V,M} = \bar{\sigma}_0 \frac{1 \pm \frac{g}{4\pi}}{1 \mp \frac{g}{4\pi}}, \quad (9)$$

TABLE I. Conductivity corrections from the first-order classes of diagrams (Fig. 1) for MLG (BLG) in corresponding  $\bar{\sigma}_0$  units (Ref. 18). MLG results are shown for  $\Lambda \gg \omega$ . Here we use the shorthands  $\alpha = g/2\pi$ ,  $\ell = \log(\Lambda/\omega)$ , and  $\beta = g/8\omega$ . The degeneracy factors for each diagram and combinatorial factor 2 are taken into account (first column).

Diagram class	Scalar disorder	Gap disorder	Vector disorder
(1, 1) $\times$ 1	$\alpha[1 + 2\ell]/2$ ( $2\beta$ )	$-\alpha[1 - 2\ell]/2$ ( $2\beta$ )	$2\alpha\ell$ ( $4\beta$ )
(1, 2) $\times$ 2	$-\alpha\ell$ ( $-2\beta$ )	$-\alpha\ell$ ( $-2\beta$ )	$-2\alpha\ell$ ( $-4\beta$ )
Total $\times$ 2	$\alpha$ (0)	$-\alpha$ (0)	0 (0)

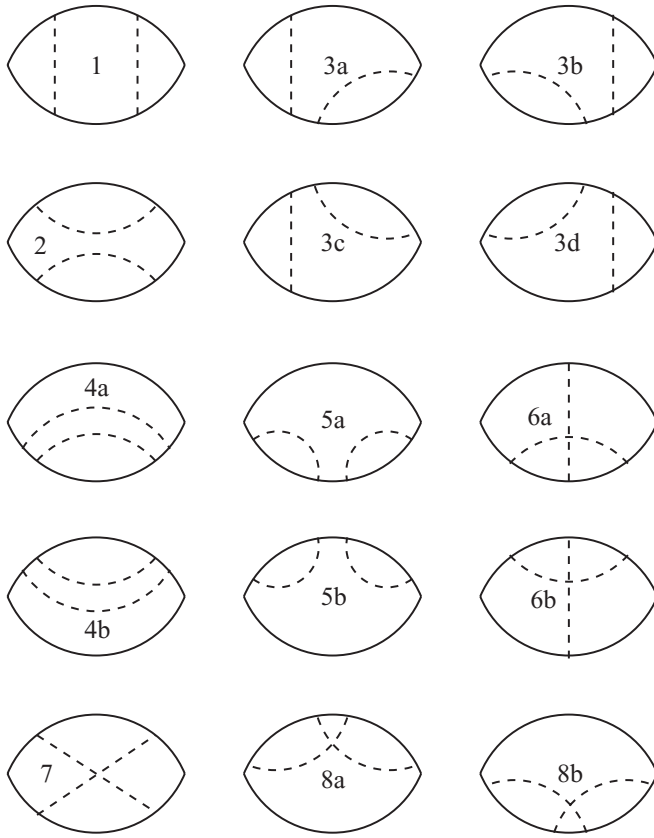


FIG. 2. Three-loop corrections of the two-particle Green's function. Each diagram appears four times. Generally, the combinatorial factor of each  $n$ th order diagram is  $2^n$ .

for random scalar potential (+) and random gap (−), correspondingly. It should be noticed that the conductivity is enhanced (reduced) by scalar-potential (gap) disorder. This is plausible because the fluctuations of the former add particles to the system at the Dirac point, whereas the latter opens a fluctuating gap that should reduce the contribution to the conductivity.

In the case of bilayer, the integral in Eq. (7) converges for  $\Lambda \rightarrow \infty$ , giving  $I \sim \text{const}$ . Therefore, corrections to the displacement function arising from each  $n$ th order diagram become proportional to  $\omega^{-2-n}$ . Formally, this leads to the

singularity  $\sim \omega^{-n}$  of each  $n$ th order conductivity correction for small  $\omega$ , as is shown in Tables I and II (values in brackets). Details of the evaluation of the first-order diagrams are summarized in Ref. 18. However, the sum over all contributions gives a zero for all disorder types in both first and second order of perturbation theory. Provided this cancellation holds to higher orders as well, the minimal conductivity of bilayer graphene turns out to be very robust with respect to all types of disorder.

*Discussion.* The conductivity formula Eq. (9) represents the main result of our work. It has the required form  $\bar{\sigma} = \bar{\sigma}_0 K_g$ . An important feature of this solution is its scale invariance. Indeed, while this expression has been obtained for a finite frequency  $\omega$  after performing the limit  $\Lambda \rightarrow \infty$ , formally, the same result follows by keeping the cutoff  $\Lambda$  finite and performing the limit  $\omega \rightarrow 0$ . Hence, Eq. (9) can be regarded as an asymptotically exact solution of the DC transport problem in disordered ML graphene.

For the particular case of the random gap disorder in MLG with zero average gap, our results confirm findings of the recent numerical works.<sup>19,20</sup> For  $g \sim 0$  it reproduces the field theoretical result obtained in Ref. 12. The robustness of the minimal conductivity for BLG for zero average mass is in remarkable agreement with the nonperturbative result obtained in Ref. 14. On the other hand, the perturbation theory fails to describe a metal-insulator transition typical for a two-dimensional electron gas.<sup>14,20</sup> This is because the scattering rate  $\eta$  vanishes in perturbation theory, whereas a nonzero  $\eta$  is the parameter which controls the metal-insulator transition according to Eq. (6). Hence, the area of applicability of perturbation theory is restricted to the metallic phase.

Apart from the contribution to the displacement function shown in Eq. (2), there are two further contributions which emerge from the Kubo formula and might become important sufficiently far away from the Dirac point.<sup>13</sup> In terms of one-particle Green's functions, they correspond to the product  $G(\pm z)G(\pm z)$ . However, close to the Dirac point these contributions can be neglected in comparison to Eq. (2). Although the reason for neglecting them is not evident from the point of view of perturbation theory, the argument is provided by the field theory. The latter demonstrates the absence of massless modes at the saddle point for these contributions,<sup>12,13</sup> i.e., at the Dirac point they are strongly suppressed and do not contribute to the transport.

TABLE II. Conductivity corrections from the second-order classes of diagrams (Fig. 2) for MLG (BLG) in corresponding  $\bar{\sigma}_0$  units. All shorthands as above. The degeneracy factors and combinatorial factor 4 are taken into account (first column).

Diagram class	Scalar disorder	Gap disorder	Vector disorder
(2, 1) $\times$ 1	$\alpha^2[1 + 4\ell + 6\ell^2]/8$ ( $3\beta^2/2$ )	$\alpha^2[1 - 4\ell + 6\ell^2]/8$ ( $3\beta^2/2$ )	$3\alpha^2\ell^2$ ( $6\beta^2$ )
(2, 2) $\times$ 1	$5\alpha^2\ell^2/12$ ( $5\beta^2/6$ )	$5\alpha^2\ell^2/12$ ( $5\beta^2/6$ )	$5\alpha^2\ell^2/3$ ( $10\beta^2/3$ )
(2, 3) $\times$ 4	$-\alpha^2\ell[1 + \ell]$ ( $-3\beta^2$ )	$-\alpha^2\ell^2$ ( $-3\beta^2$ )	$-2\alpha^2\ell[1 + 2\ell]$ ( $-12\beta^2$ )
(2, 4) $\times$ 2	$\alpha^2\ell[1 - \ell]/2$ ( $2\beta^2/3$ )	$\alpha^2\ell[1 - \ell]/2$ ( $2\beta^2/3$ )	$2\alpha^2\ell[1 - \ell]$ ( $8\beta^2/3$ )
(2, 5) $\times$ 2	$\alpha^2\ell^2/3$ (0)	$\alpha^2\ell^2/3$ (0)	$4\alpha^2\ell^2/3$ (0)
(2, 6) $\times$ 2	0	0	0
(2, 7) $\times$ 1	0	0	0
(2, 8) $\times$ 2	0	0	0
Total $\times$ 4	$\alpha^2/2$ (0)	$\alpha^2/2$ (0)	0

In conclusion, we have carefully studied perturbative corrections to the conductivity of disordered monolayer and bilayer graphene for different disorder types. Up to three-loop order we managed to show that in the case of ML graphene logarithmic divergences cancel each other exactly, irrespectively of the disorder type. Thus, the conductivity of weakly disordered monolayer graphene is modified by a finite

correction. On the other hand, the minimal conductivity of bilayer graphene does not acquire any corrections for any type of disorder, as we have demonstrated for the first and second order in the perturbative expansion.

We acknowledge financial support by the DFG Grant No. ZI 305/5-1.

- 
- <sup>1</sup>K. S. Novoselov, A. K. Geim, S. V. Morozov, D. Jiang, M. I. Katsnelson, I. V. Grigorieva, S. V. Dubonos, and A. A. Firsov, *Nature (London)* **438**, 197 (2005).
- <sup>2</sup>K. S. Novoselov, E. McCann, S. V. Morozov, V. I. Fal'ko, M. I. Katsnelson, U. Zeitler, D. Jiang, F. Schedin, and A. K. Geim, *Nat. Phys.* **2**, 177 (2006).
- <sup>3</sup>M. I. Katsnelson, K. S. Novoselov, and A. K. Geim, *Nat. Phys.* **2**, 620 (2006).
- <sup>4</sup>Y. Zhang, Y.-W. Tan, H. L. Stormer, and P. Kim, *Nature (London)* **438**, 201 (2005).
- <sup>5</sup>T. Ohta, A. Bostwick, T. Seyller, K. Horn, and E. Rotenberg, *Science* **313**, 951 (2006).
- <sup>6</sup>A. K. Geim and K. S. Novoselov, *Nat. Mater.* **6**, 183 (2007).
- <sup>7</sup>Y.-W. Tan, Y. Zhang, K. Bolotin, Y. Zhao, S. Adam, E. H. Hwang, S. Das Sarma, H. L. Stormer, and P. Kim, *Phys. Rev. Lett.* **99**, 246803 (2007).
- <sup>8</sup>S. V. Morozov, K. S. Novoselov, M. I. Katsnelson, F. Schedin, D. C. Elias, J. A. Jaszczak, and A. K. Geim, *Phys. Rev. Lett.* **100**, 016602 (2008).
- <sup>9</sup>J. H. Chen, C. Jang, M. S. Fuhrer, E. D. Williams, and M. Ishigami, *Nat. Phys.* **4**, 377 (2008).
- <sup>10</sup>E. Fradkin, *Phys. Rev.* **33**, 3257 (1986); **33**, 3263 (1986).
- <sup>11</sup>A. W. W. Ludwig, M. P. A. Fisher, R. Shankar, and G. Grinstein, *Phys. Rev. B* **50**, 7526 (1994).
- <sup>12</sup>K. Ziegler, *Phys. Rev. B* **55**, 10661 (1997); K. Ziegler and G. Jug, *Z. Phys. B* **104**, 5 (1997); K. Ziegler, *Phys. Rev. Lett.* **80**, 3113 (1998).
- <sup>13</sup>K. Ziegler, *Phys. Rev. B* **78**, 125401 (2008).
- <sup>14</sup>K. Ziegler, *Phys. Rev. Lett.* **102**, 126802 (2009); *Phys. Rev. B* **79**, 195424 (2009).
- <sup>15</sup>A. Sinner, A. Sedrakyan, and K. Ziegler, *Phys. Rev. B* **83**, 155115 (2011).
- <sup>16</sup>A. Giuliani, V. Mastropietro, and M. Porta, *Phys. Rev. B* **83**, 195401 (2011).
- <sup>17</sup>D. S. L. Abergel, V. Apalkov, J. Berashevich, K. Ziegler, and T. Chakraborty, *Adv. Phys.* **59**, 261 (2010).
- <sup>18</sup>See Supplemental Material at <http://link.aps.org/supplemental/10.1103/PhysRevB.84.233401> for calculational details of the diagrams.
- <sup>19</sup>J. H. Bardarson, M. V. Medvedyeva, J. Tworzydło, A. R. Akhmerov, and C. W. J. Beenakker, *Phys. Rev. B* **81**, 121414(R) (2010).
- <sup>20</sup>M. V. Medvedyeva, J. Tworzydło, and C. W. J. Beenakker, *Phys. Rev. B* **81**, 214203 (2010).